Analysis of gamma-ray spectra with spectral unmixing - Part I: Determination of the characteristic limits (decision threshold and statistical uncertainty) for measurements of environmental aerosol filters

Jiaxin Xu, Jérôme Bobin, Anne de Vismes Ott, Christophe Bobin, Paul Malfrait

Analysis of gamma-ray spectra with spectral unmixing — Part I: Determination of the characteristic limits (decision threshold and statistical uncertainty) for measurements of environmental aerosol filters

Jiaxin Xu[a], Jérôme Bobin[b,*], Anne de Vismes Ott[a], Christophe Bobin[c], Paul Malfrait[a]

[a]*IRSN/LMRE, Rue du Belv´ed`ere, 91400 Orsay, France*
[b]*CEA IRFU/DEDIP, 91191 Gif-sur-Yvette, France*
[c]*CEA, LIST, Laboratoire national Henri Becquerel, (LNE-LNHB), 91191 Gif-sur-Yvette Cedex, France*

Abstract

Poisson-statistics based spectral unmixing has previously been shown to be an efficient analysis tool for the activity estimation of radionuclides from gamma-ray spectroscopy measurements. In this paper, we present the quantification of characteristic limits (decision threshold, detection limit and limits of the coverage interval) for the metrological use of such spectral unmixing algorithms. The proposed approaches are evaluated and validated with simulated spectra of HPGe and NaI measurements by comparing the results to characteristic values calculated from Monte Carlo simulations.

Keywords: gamma-ray spectrometry, characteristic limits, full spectrum analysis, spectral unmixing

1. Introduction

The gamma-ray spectrum analysis problem has been tackled with spectral unmixing in Xu et al. (2020), Paradis et al. (2020). These studies show that such new algorithms based on the full spectrum analysis and the Poisson statistics underlying the gamma-ray detection process provides a more sensitive analysis of radionuclides than standard peak-based algorithms. In this work, we focus on the metrological use of the spectral unmixing algorithms, which further ne-

Corresponding author
Email address: jerome.bobin@cea.fr (Jérôme Bobin)

cessitates quantifying the characteristic limits associated with the measurement result.

The characteristic limits generally consist of the decision threshold, the detection limit and limits of the coverage interval, are essential for decision making purposes of the measurement results. While the calculation of these limits have been well studied in peak-based analysis, new calculation approaches are needed for the spectral unmixing algorithms due to their different estimation procedures. More, precisely, contrast to peak-based algorithms, the spectral unmixing is an analysis tool that identifies and quantifies radionuclides from the full energy spectrum (*i.e.*, peaks and their associated continua) of a gamma-ray measurement. The problem can be generally written in the matrix formulation as follows :

$$\boldsymbol{x} \sim \mathcal{P}oisson\left(\boldsymbol{\Phi a} + \boldsymbol{b}\right) \tag{1}$$

With the aim of decomposing a measured spectrum $\boldsymbol{x} \in \mathbb{R}^{M\times 1}$ (composed of M channels) into a linear combination of radionuclides' spectral signatures $\boldsymbol{\Phi} \in \mathbb{R}^{M\times N}$ (containing N radionuclides' spectral signatures) and a background spectrum $\boldsymbol{b} \in \mathbb{R}^{M\times 1}$, the spectral unmixing estimates radionuclides' mixing weights $\boldsymbol{a} \in \mathbb{R}^{N\times 1}$ that are proportional to radionuclides' activities. Therefore, we focus on the calculation of characteristic limits of the mixing weights estimated with Poisson-statistics based spectral unmixing algorithms.

The paper is organized as follows: Section 2 presents the concept of characteristic limits for radioactivity measurements. In Section 3, we describe the data used in this work and present how the characteristic limits can be calculated from Monte Carlo simulations. Section 4.2 explores the calculation of the decision threshold. Next, we discuss the assessment of the coverage intervals in Section 5. Section 6 provides conclusions of this work.

2. Characteristic limits in radioactivity measurements

Refer to ISO 11929, the notations below are used in the description of the characteristic limits:

- Y: Measurand, the quantity of interest.
- y: Determined value of the measurand Y (*i.e.*, the estimate of Y).
- $\tilde{y}$: True value of the measurand.

We first present the classical statistical hypothesis framework used for decision making in gamma-ray spectrum analysis. It is commonplace to consider testing hypotheses with the two alternatives (associated with type I error and type II error described in Table 1):

- H_0: the null hypothesis, where a given radionuclide is not "active".
- H_1: the alternate hypothesis, where the radionuclide is present in the mixture.

	H_0 is true	H_1 is true
rejecting H_0	**Type I error**: the error of rejecting H_0 when it is true, the probability of committing a type I error is denoted by α, called false positive rate.	
accepting H_0		**Type II error**: the error of accepting H_0 when H_1 is true, the probability of committing a type II error is denoted by β, called false negative rate.

Table 1: Two types of errors of hypotheses test.

The standardization document ISO 11929 defines the determination of the characteristic limits, namely the decision threshold, the detection limit, and limits of the coverage interval for ionizing radiation measurements. It provides a framework for the computation of the characteristic limits. Referring to Weise

et al. (2005), Michel (2016), the definition and interpretation of the characteristic limits for some estimate y of a measurand Y are as follows:

- **Decision threshold (DT)** allows a decision to be made on whether or not the physical effect quantified by the measurand is present.

  The determination of DT is related to the Type I error described in Table 1. When the quantity y exceeds the critical value (DT), the null hypothesis H_0 should be rejected with respect to a given false positive rate (FPR). It can be described with:

  $$\alpha = \mathcal{P}\left(y \geq DT | \tilde{y} = 0\right) \tag{2}$$

  where $\tilde{y}$ is the true value of the measurand and α is the desired critical FPR.

- **Detection limit (DL)** indicates the smallest true quantity value of the measurand, which can still be detected with the applied measurement procedure.

  The determination of DL is related to the Type II error described in Table 1. It is selected with respect to a desired false negative rate (FNR) based on the decision threshold level.

  More precisely, the detection limit (DL) is the smallest value that provides a desired Type II error probability β:

  $$\beta = \mathcal{P}\left(y \leq DT | \tilde{y} = DL\right) \tag{3}$$

  where the DT is given and $\tilde{y}$ is the true value of the measurand.

- **The coverage interval** for the estimate y is an interval that has a probability γ of containing the true value $\tilde{y}$.

3. Data description and the characteristic limits assessment with Monte Carlo simulations

In this work, the investigations are based on the following gamma-ray spectra simulations:

- Simulated aerosol filter measurement of an HPGe detector cylindrical (60 %relative efficiency) Xu et al. (2020), which corresponds to the energy response of gamma-emitting radionuclides from 20 keV to 1640 keV composed in 16384 channels. This mixing scenario consists of 10 radionuclides: ^{7}Be, ^{22}Na, ^{40}K, ^{137}Cs, ^{210}Pb, ^{208}Tl, ^{212}Bi, ^{212}Pb, ^{214}Bi, ^{214}Pb. Their mixing weights are fixed to values that are customary in real aerosol measurements.

  In this context we focus on the assessment of characteristic limits for 4 radionuclides: ^{7}Be, ^{22}Na, ^{137}Cs, ^{212}Pb, since these radionuclides cover the whole energy range and different statistic regimes. The simulation model of 10 radionuclides and the contribution of these 4 radionuclides are displayed in Figure 1.

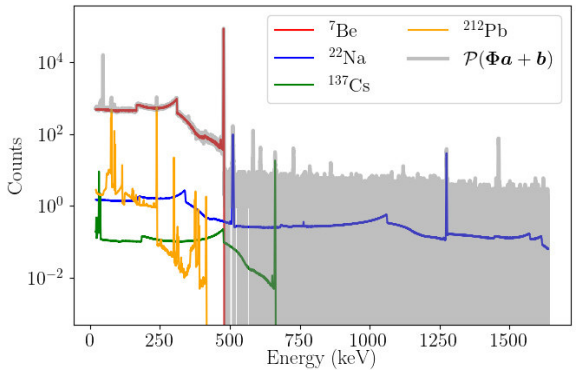

Figure 1: Spectral unmixing model used to illustrate the evaluation of the characteristic limits. The simulated measurements (gray) are composed of the above 10 radionuclides, while individual spectra of ^{7}Be,^{22}Na,^{137}Cs,^{212}Pb will be evaluated.

- Simulated measurements of a 3"x3" NaI(Tl) detector without shielding using point sources placed at a distance of 1 m Paradis et al. (2020), which is made of 1024 channels. The spectral signatures correspond to the detector response of 4 gamma-emitting radionuclides with photon emissions covering a range of energies between 40 keV and 2 MeV: ^{60}Co, ^{134}Cs, ^{137}Cs,

^{152}Eu (see Figure 2).

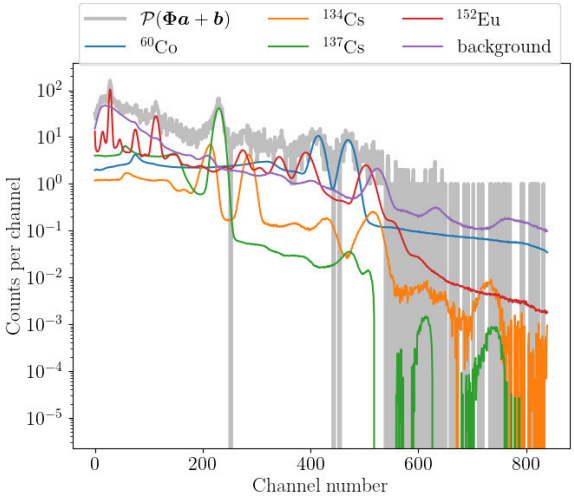

Figure 2: Spectral unmixing model of simulations of NaI measurements.

A traditional approach to quantify the characteristic limits for some estimation method is to make use of Monte-Carlo simulations. In the following paragraphs, we present how the characteristic limits of the spectral unmixing method can be calculated from Monte Carlo simulations.

Decision threshold from Monte Carlo simulations. Monte Carlo simulations that mimic the mixture under the null hypothesis of a radionuclide allows quantifying the false positive rate of this radionuclide, thus the decision threshold. For each radionuclide, 1000 simulations are performed with this radionuclide set to zero and other radionuclides set to their actual levels. The spectral unmixing algorithm is subsequently applied to estimate radionuclides' mixing weights from these simulated spectra. The distribution of the estimated mixing weight of this radionuclide allows computing a decision threshold with respect to some false positive rate from the according percentile of the distribution.

Coverage interval from Monte Carlo simulations. In practice, and assuming that some estimate of the mixing weights have a limited estimation bias

or error, a coverage interval with respect to a given probability γ and for individual radionuclides can be derived by performing Monte-Carlo simulations. More precisely, we first perform 1000 Monte Carlo simulations that mimic the actual mixing scenario of radionuclides. Next, the spectral unmixing algorithm is applied to estimate mixing weights from these simulated spectra. Finally, the coverage intervals of radionuclides can be derived from the distribution of their estimated mixing weights.

In practice, Monte Carlo simulations are seldom used to analyze gamma-ray spectra in routine analysis procedures. The main drawback is their massive computational cost since Monte Carlo simulations are needed for each new spectrum to be analyzed. In the next sections, we focus on computationally cheaper and yet precise alternatives to derive the characteristic limits without resorting to Monte-Carlo simulations.

4. Quantifying the decision threshold

4.1. Decision threshold in peak-based analysis

In gamma-ray spectrum analysis, the decision threshold is usually derived from some statistical test based on the measured spectrum. This amounts to evaluating how much the estimated quantity associated with a radionuclide's activity departs from the background (*i.e.*, other contributions composed in the measured spectrum) and is therefore statistically consistent or not with this background.

In the peak-based analysis, the activity is associated with the net counts. It is the total number of counts measured in a given ROI, which further corrected by the average number of counts of the background:

$$N_n = N_g - N_0 \tag{4}$$

where N_n is the net counts number associated to the activity, N_g is the observed gross number of counts and N_0 is the number of background counts.

Recall the definition of DT in Section 2, the DT level of the measurand (*i.e.*, net counts number) is derived from:

$$\alpha = \mathcal{P}(N_n \geq DT | \tilde{N_n} = 0) \tag{5}$$

where α and $\tilde{N_n}$ stands for the desired FPR and the true value of the net number of counts respectively. The estimated number of N_g and N_0, noted $\hat{N_g}$ and $\hat{N_0}$ respectively. In practice, the DT is derived from some statistical test of the quantity $\hat{N_g} - \hat{N_0}$ under the hypothesis of $\tilde{N_n} = 0$, which has:

- mean value equal to zero.
- variance according to $2\hat{N_0}$, since both of N_g and N_0 follow the Poisson statistic thus their mean value are equal to their variance, and $N_g = N_0$ under the hypothesis of $\tilde{N_n} = 0$.

4.2. Decision threshold in spectral unmixing analysis

The DT determination in peak-based analysis considers that the background spectrum N_0 is well estimated and provides a mean value of the distribution under the null hypothesis, from which the DT can be derived based on a desired FPR. Now, we aim to investigate the DT in the spectral unmixing approach, where the measurand associated with a radionuclide's activity is the number of counts in the full spectrum range. The DT can be derived with the same idea of statistical test based on a "background", but adapted to the full spectrum analysis.

Recall that the spectral unmixing decomposes a gamma-ray spectrum into individual spectra of radionuclides. To determine the decision threshold of a single radionuclide indexed by j in the unmixing model, we reformulate the true linear mixing model with this radionuclide and an equivalent background:

$$\boldsymbol{\Phi a} + \boldsymbol{b} \rightarrow \boldsymbol{\phi}_j a_j + \boldsymbol{m} \tag{6}$$

where $\boldsymbol{\phi}_j a_j$ represents the individual spectrum of the j^{th} radionuclide, while the other radionuclides and the background spectrum $\boldsymbol{b}$ compose an equivalent

background:

$$\boldsymbol{m} = \sum^{l \neq j} \boldsymbol{\phi}_l a_l + \boldsymbol{b}$$

In the spectral unmixing analysis, the activity of the j^{th} radionuclide is associated to the mixing weight a_j. Recall the definition in Section **??**, the DT level of the measurand (*i.e.*, a_j) is derived from:

$$\alpha = \mathcal{P}\left(a_j \geq DT | \tilde{a}_j = 0\right) \tag{7}$$

Recall that, the measured spectrum $\boldsymbol{x}$ is composed of M channels, $\forall i \in [1, ..., M]$, the observed counts in each channel of the spectrum follows a Poisson distribution with mean value: $\lambda_i = [\boldsymbol{\phi}_j a_j]_i + m_i$.

The DT can be derived from a standard hypothesis testing procedure test under the null alternative of $H_0 : \tilde{a}_j = 0$, which leads to $\lambda_i = m_i$ for $\forall i \in M$. This can be generally formulated with some statistical test T as follows:

$$\alpha = \mathcal{P}\big(T \geq T(\lambda) | \forall i, \lambda_i = m_i\big) \tag{8}$$

For this purpose, we propose to make use of statistical test based on different assumptions as follows:

a. Test based on the sum of observed counts:. a simple statistical test to consider is based on the total number of counts, as measured by the sum of observed counts under the null hypothesis H_0. Thanks to the statistical independence of each channel, this quantity should follow a Poisson distribution with mean value $\hat{\boldsymbol{m}}$ (*i.e.*, estimated equivalent background).

$$\sum_i x_i \sim \mathcal{P}oisson\left(\sum_i \hat{m}_i\right) \tag{9}$$

Therefore, the DT (noted a_j^*) of the estimated activity for the j^{th} radionuclide with a given false positive rate α, can be derived from the cumulative distribution function (CDF) of the following distribution:

$$\alpha = \mathcal{P}\Big(\sum_{i \in C} x_i \geq \sum_{i \in C} [\boldsymbol{\phi}_j a_j^*]_i + \sum_{i \in C} m_i\Big) \tag{10}$$

where C is some set of observed channels. The total number of counts from the full spectrum is a special case where C defines all the observed channels. While it allows to account for the full information carried out by the spectrum, it however poorly distinguishes the radionuclide to be tested from the background. We rather use the pre-specified channels in a region of interest, where the equivalent background is better distinguished from the j^{th} radionuclide. (*e.g*, peak region of the radionuclide).

b. Test based on sum of weighted observed counts:. In order to better distinguish between the radionuclide to be tested and the equivalent background, we further investigate statistical test derived from the sum of weighted counts in different channels written as $\sum_i w_i m_i$ with the following choice of w_i:

- Let $\boldsymbol{\Psi} = \begin{bmatrix} \boldsymbol{\phi}_j & \boldsymbol{m} \end{bmatrix}$, the least squares solution of the mixing vector of $\boldsymbol{\Psi}$ can be written as:

$$\hat{\boldsymbol{a}} \in \underset{\boldsymbol{a}}{\operatorname{argmin}} \frac{1}{2} \|\boldsymbol{x} - \boldsymbol{\Psi a}\|^2 \tag{11}$$

for which the solution is $\hat{\boldsymbol{a}} = \boldsymbol{\Psi}^\dagger \boldsymbol{x}$, where $\boldsymbol{\Psi}^\dagger = (\boldsymbol{\Psi}^T \boldsymbol{\Psi})^{-1} \boldsymbol{\Psi}^T$ is the pseudo inverse matrix.

We make use of the the component of $\boldsymbol{\Psi}^\dagger$ related to $\boldsymbol{\phi_j}$ as the weights matrix, noted as $\boldsymbol{w}_1 = \boldsymbol{\Psi}^\dagger_\phi$. As graphically illustrated in Figure 3, it allows projecting onto the span of $\boldsymbol{\phi}_j$ parallelly to $\boldsymbol{m}$.

Nevertheless, the resulting statistical test do not follow a Poisson distribution. Thankfully, since it is defined as a linear combination of a large number of observed channels, one can approximate the distribution to be Normal. The resulting statistical test with observed counts $\boldsymbol{x}$ and estimated equivalent background $\boldsymbol{m}$ will be carried out as follows:

$$\sum_i w_i x_i \sim \mathcal{N}\left(\sum_i w_i m_i, w_i^2 m_i\right) \tag{12}$$

while in each channel, the mean value $\mu = w_i m_i$ and variance $\sigma^2 = w_i^2 m_i$ are considered, since both the mean value and the variance of the model equal to m_i because of the Poisson statistics.

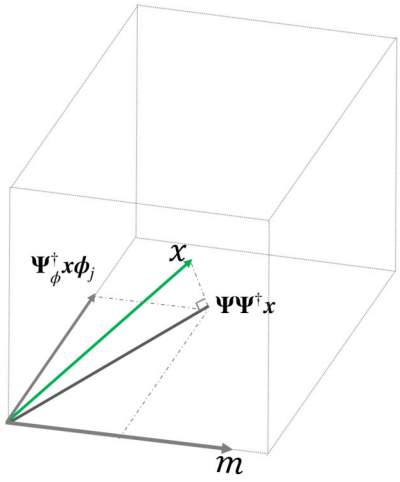

Figure 3: Schema of the least squares solution of the equivalent background model.

The DT of the estimated activity a_j^* can be derived from the CDF of Normal distribution:

$$\frac{\alpha}{2} = \mathcal{P}\Big(\sum_i w_i x_i \geq \sum_i w_i [\boldsymbol{\phi}_j a_j^*]_i + \sum_i w_i m_i\Big) \tag{13}$$

- the weighted background statistical test is further studied with $\boldsymbol{w}_2 = \boldsymbol{\Psi}_{\phi}^{\dagger}$ with:

$$\boldsymbol{\Psi}^{\dagger} = \Big(\boldsymbol{\Psi}^T \mathrm{diag}(\frac{1}{\boldsymbol{\phi}_j a_j + \boldsymbol{m}})\boldsymbol{\Psi}\Big)^{-1} \boldsymbol{\Psi}^T \mathrm{diag}\big(\frac{1}{\boldsymbol{\phi}_j a_j + \boldsymbol{m}}\big) \tag{14}$$

4.3. Evaluation of the decision threshold determination

For a comparison purpose, by fixing the false positive rate to $\alpha = 2.5\%$, we evaluate the statistical tests proposed in Section 4.2 to assess the decision threshold for HPGe and NaI measurements described in Section 3, while the results are compared to those carried out with Monte Carlo simulations. The evaluations are carried out as follows:

- For each radionuclide, the accurate DT level quantified with respect to $1-\alpha$ percentile of the distribution of estimated values from Monte Carlo simulations under the null hypothesis of this radionuclide.

- Decision threshold assessment with different statistical tests for each Monte Carlo simulation:

  - the Poisson statistical test based on the sum of counts in peak region. This is used only for HPGe measurements since using the peak regions to analyze NaI measurements is not interesting due to the correlations of spectra, for which it is better to take into account the full spectrum information. Experiments on the described mixing scenario (see Figure 1) of the HPGe measurement considers the following peak regions: ^{7}Be at 477 keV, ^{22}Na at 1274 keV, ^{137}Cs at 661 keV and ^{212}Pb at 238 keV.

  - the Gaussian statistical test based on two choices of weighted sum of counts, noted $\boldsymbol{w}_1$ and $\boldsymbol{w}_2$ respectively.

Results

For HPGe spectra, the different statistical tests are compared in Figure 4, 5, 6 and 7. Figure 8, 9, and 10, and 11 for NaI spectra respectively. The results report the distribution of:

- Poisson test based on region of interest (ROI) (green) of $\boldsymbol{x}$.
- Gaussian test based on sum of weighted counts carried out by $\boldsymbol{w}_1\boldsymbol{x}$ (blue) and $\boldsymbol{w}_2\boldsymbol{x}$ (orange).
- For a comparison purpose, the accurate DT level calculated from Monte Carlo (*i.e.*, $1-\alpha$ percentile of the distribution under the null hypothesis) is displayed with a dotted line (red).

From these results, we can draw the following conclusions:

- Firstly, compared to the Gaussian statistical test based on the sum of weighted counts, the Poisson statistical test based on the sum of the counts in the ROI is less efficient to derive the DT. Since the peaks are not well distinguished from the continua.

- For HPGe measurement, for ^{22}Na, ^{137}Cs and ^{212}Pb, the Gaussian statistical test of weighted counts with w_2 derives similar DT levels comparing to the actual $1-\alpha$ percentile of the distribution (*i.e.*, accurate DT level), which is better than the choice of w_1. This is not valid for ^{7}Be due to the fact that ^{7}Be is predominant in the measured spectrum, while its equivalent background is poorly estimated. However, the determination of accurate DT level for low-level radionuclides is more important for the decision making purpose; in such case, the dominant spectral contribution such as ^{7}Be can provide a better estimation of the equivalent background thus more accurate DT determination for low-level radionuclides.

- When we further focus on the results of NaI measurements, the choice of using w_2 is shown to be more consistent than w_1; it allows better distinguishing a radionuclide from its equivalent background when the spectra are overlapped in the whole energy range.

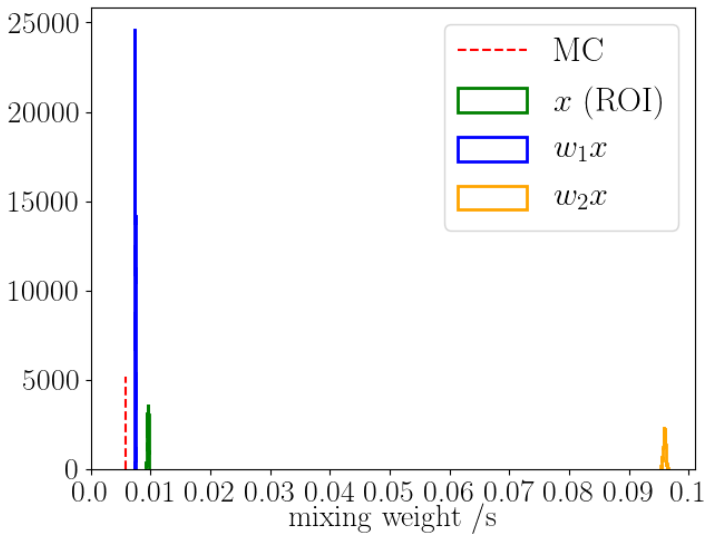

Figure 4: DT assessment for HPGe measurements: ^{7}Be

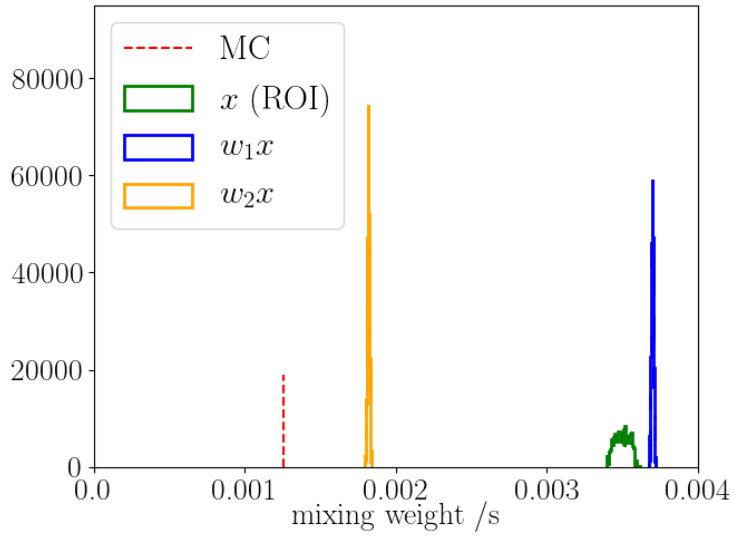

Figure 5: DT assessment for HPGe measurements: ^{22}Na

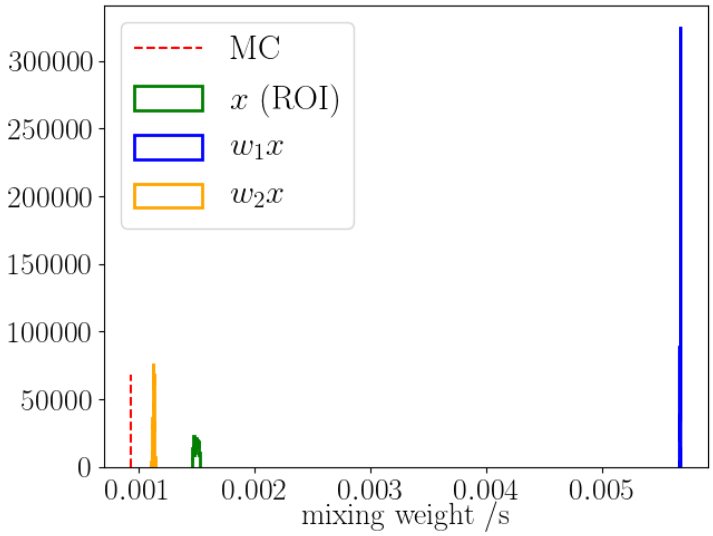

Figure 6: DT assessment for HPGe measurements: ^{137}Cs

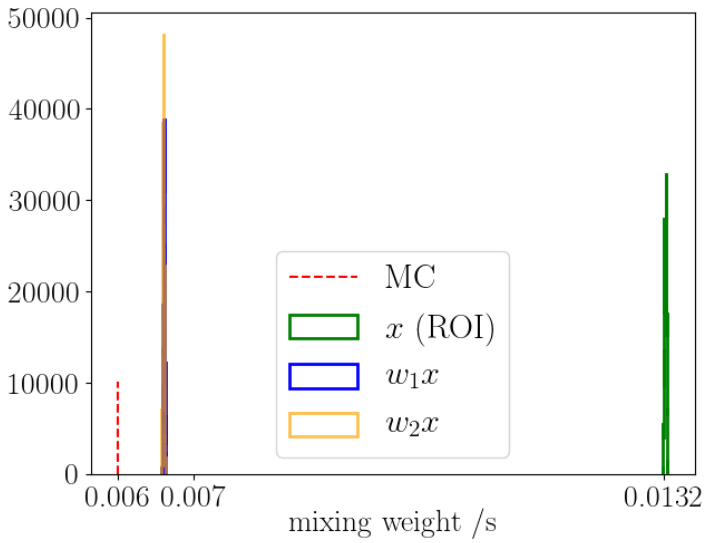

Figure 7: DT assessment for HPGe measurements: ^{212}Pb

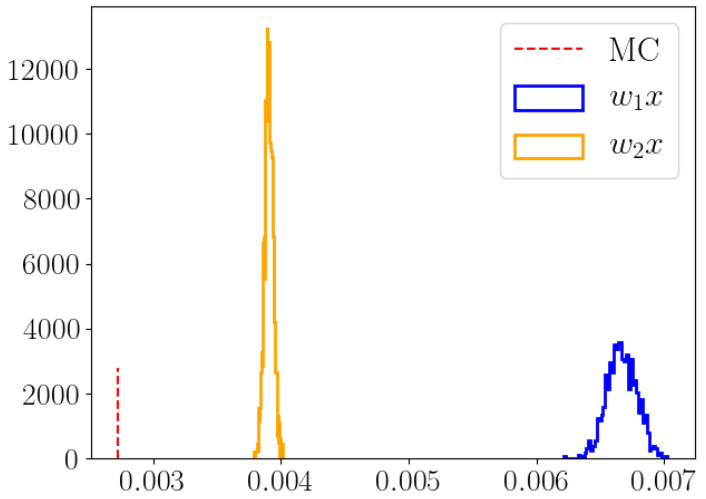

Figure 8: DT assessment for NaI measurements: ^{60}Co

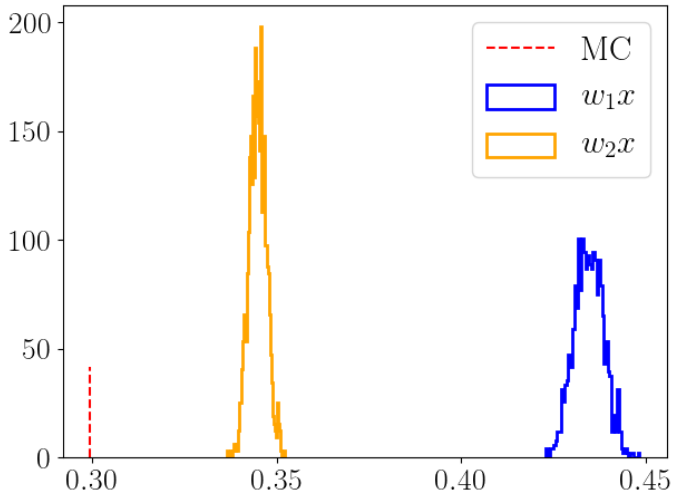

Figure 9: DT assessment for NaI measurements: ^{134}Cs

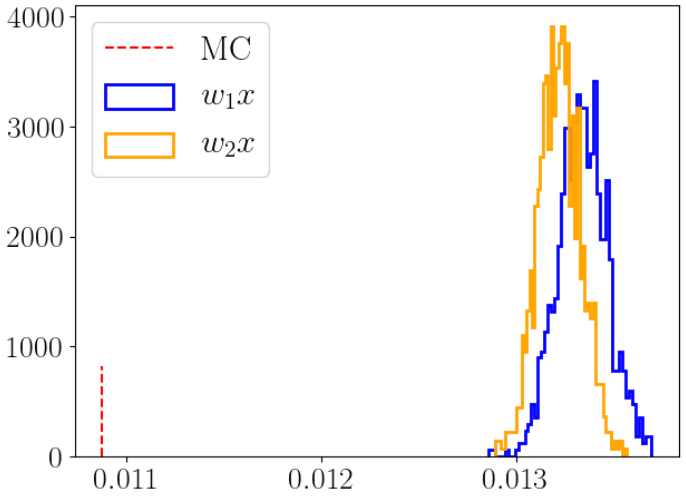

Figure 10: DT assessment for NaI measurements: ^{137}Cs

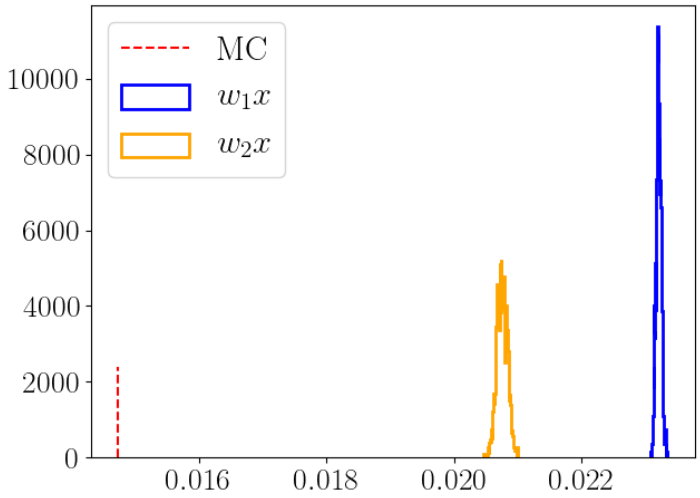

Figure 11: DT assessment for NaI measurements: ^{152}Eu

5. Confidence interval

The statistical uncertainty of the estimation of a parameter is twofold: the estimation bias and an interval of values that contains the true value of the parameter. In the spectral unmixing approach, the assessment of uncertainties can be carried out from Monte Carlo simulations that mimic the actual mixture of radionuclides as presented in Section 3. The distribution of estimated values provides both the estimation bias and the coverage interval. However, this requires a massive amount of simulations, making this approach hard to implement in practice. Nevertheless, the Poisson-based spectral unmixing is shown to provide accurate activity estimations; we can only focus on determining a coverage interval from the estimated mixing weights.

5.1. Fisher information to compute coverage intervals

For the observed variable x distributed as $f(x|\theta)$, the maximum likelihood estimator (MLE) can be approximated with a Gaussian distribution:

$$\mathcal{N}\left(\theta, I(\theta)^{-1}\right) \tag{15}$$

where $I(\theta)$ is the Fisher information (Fisher (1956)) defined as:

$$I(\theta) = \mathbb{E}_\theta \left[\frac{\partial^2 \log f(x|\theta)}{\partial \theta^2} \right] \tag{16}$$

The estimation standard error can be obtained by replacing the unknown true value θ by the estimated value $\hat{\theta}$.

In our activity estimation problem, the investigated Poisson-based spectral unmixing provides a maximum likelihood estimate of the mixing weights, noted $\hat{\boldsymbol{a}}$. According to the Poisson likelihood, the Fisher information matrix can be written as:

$$I(\hat{\boldsymbol{a}}) = \boldsymbol{\Phi}^T \mathrm{diag}\big(\boldsymbol{x} \oslash (\boldsymbol{\Phi}\hat{\boldsymbol{a}} + \boldsymbol{b})^2\big)\boldsymbol{\Phi} \tag{17}$$

We propose to assess the coverage interval of the estimated mixing weights $\hat{\boldsymbol{a}}$ by the diagonal elements of $\sqrt{I(\hat{\boldsymbol{a}})^{-1}}$, which approximates the standard deviation of the distribution.

5.2. Evaluation of coverage interval in spectral unmixing

In this paragraph, the coverage interval assessment with Fisher information matrix is evaluated with simulations of HPGe and NaI measurements described in the previous section. More precisely, we calculate the standard deviation from the Fisher information matrix and evaluate the results with Monte Carlo simulations.

Firstly, we make use of the Q-Q (quantile-quantile) plots, which compares the distribution of estimated activities of Monte Carlo simulations to the distribution generated from the standard deviation carried out with Fisher information. The aim is to i), test the normality of the estimator, which allows validating the coverage interval with a standard uncertainty in terms of Normal distribution. ii), compare the distribution to those obtained with Fisher information.

More precisely, for each radionuclide, we show the Q-Q plot for two data samples noted A_1 and A_2:

- A_1 for estimated activity values of Monte Carlo simulations.

- A_2 for Normal distribution generated from the Fisher information of the estimation:

$$\mathcal{N}\left(a_0, \sigma_f^2\right)$$

where a_0 is the expected mixing weight of the radionuclide and σ_f is the standard uncertainty calculated from the Fisher information matrix.

For each value a in a sample (A_1 and A_2), quantiles are calculated with:

$$\boldsymbol{q} = \frac{\boldsymbol{a} - \mu}{\sigma} \tag{18}$$

where μ and σ are the mean value and the standard deviation of the given sample.

The Q-Q plots shown in Figure 12 and Figure 13 for the HPGe measurement and the NaI measurement, respectively, display the quantiles of A_2 (Fisher quantiles) as a function of A_1 (Estimation distribution quantiles).

Firstly, the results show the normality of activity estimation of Monte Carlo simulations with the straight line of the Q-Q plots and absolute values from 0 to 3. This confirms that the coverage interval of the estimation can be carried out with an approximation of the Normal distribution. Secondly, the Normal distribution generated with spectral unmixing (Maximum likelihood estimation) and Fisher information matrix provides similar coverage intervals comparing to the real Monte Carlo distribution. To further valid this conclusion, we calculate the percentage of the values estimated from Monte Carlo simulations within the interval of:

$a_0 \pm \sigma_f$, $a_0 \pm 2\sigma_f$ and $a_0 \pm 3\sigma_f$,

where a_0, σ_f stand for the expected mixing weight (*i.e.*, simulated value) and standard error determined by the Fisher matrix. These percentage values are expected to be 68.27 %, 95.45 % and 99.73 % for normal distribution. The results are shown in Table 2 and Table 3 for HPGe and NaI measurements respectively.

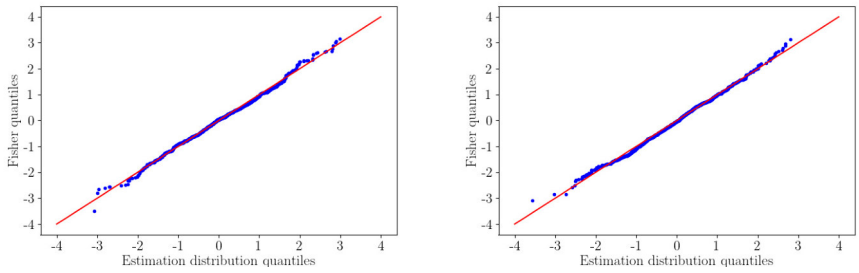

(a) ^{7}Be (b) ^{22}Na

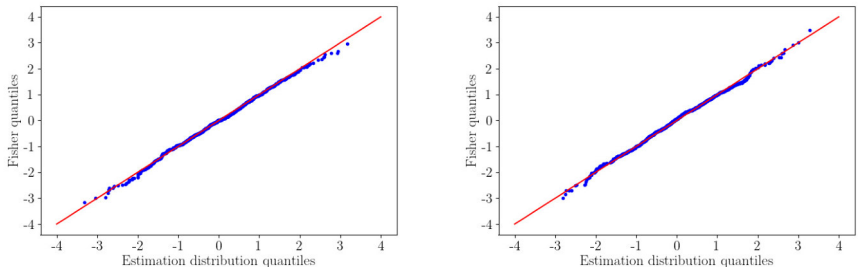

(c) ^{137}Cs (d) ^{212}Pb

Figure 12: Evaluation for the HPGe simulation: the Q-Q plots for Fisher quantiles versus estimation distribution quantiles for radionuclides.(blue). The theoretical Q-Q plots are shown in red.

	^{7}Be	^{22}Na	^{137}Cs	^{212}Pb
percentage within $a_0 \pm \sigma_f$	68.0	66.1	68.6	68.4
percentage within $a_0 \pm 2\sigma_f$	96.4	93.9	95.7	95.0
percentage within $a_0 \pm 3\sigma_f$	99.9	99.8	99.8	99.9

Table 2: Standard deviation from Fisher information matrix comparing to Monte Carlo simulations (HPGe measurements).

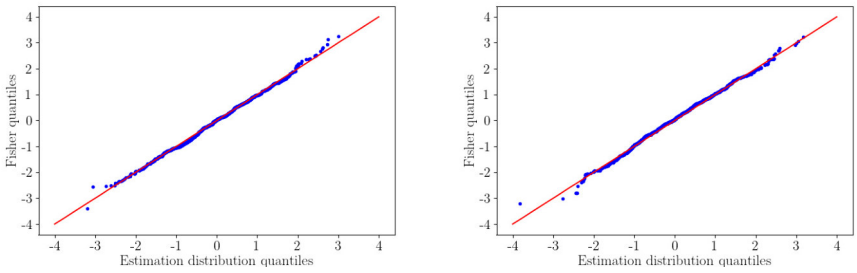

(a) ^{60}Co (b) ^{134}Cs

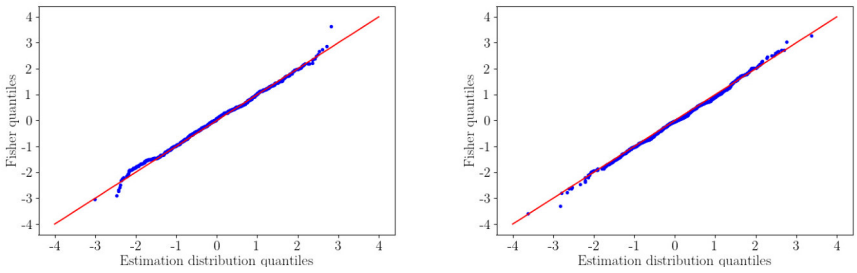

(c) ^{137}Cs (d) ^{152}Eu

Figure 13: Evaluation for the NaI simulation: the Q-Q plots for Fisher quantiles versus estimation distribution quantiles for radionuclides.(blue). The theoretical Q-Q plots are shown in red.

	^{60}Co	^{134}Cs	^{137}Cs	^{152}Eu
percentage within $a_0 \pm \sigma_f$	68.1	66.0	67.5	66.2
percentage within $a_0 \pm 2\sigma_f$	95.3	95.0	94.0	95.5
percentage within $a_0 \pm 3\sigma_f$	99.7	99.5	99.9	99.8

Table 3: Standard deviation from Fisher information matrix comparing to Monte Carlo simulations (NaI measurements).

6. Conclusion

7. Bibliography styles

References

Fisher RA. Statistical methods and scientific inference. Oliver and Boyd, 1956.

ISO 11929. Determination of the characteristic limits (decision threshold, detection limit and limits of the confidence interval) for measurements of ionizing radiation — fundamentals and application. 2010.

Michel R. Measuring, estimating, and deciding under uncertainty. Applied Radiation and Isotopes 2016;109:6–11. URL: http://www.sciencedirect.com/science/article/pii/S0969804315303626. doi:https://doi.org/10.1016/j.apradiso.2015.12.013.

Paradis H, Bobin C, Bobin J, Bouchard J, Lourenço V, Thiam C, André R, Ferreux L, de Vismes Ott A, Thévenin M. Spectral unmixing applied to fast identification of γ-emitting radionuclides using NaI(Tl) detectors. Applied Radiation and Isotopes 2020;158:109068.

Weise K, Hübel K, Michel R, Rose E, Schläger M, Schrammel D, Täschner M. Determination of the detection limit and decision threshold for ionizing-radiation measurements: fundamentals and particular applications 2005;ISSN 1013-4506.

Xu J, Bobin J, de Vismes Ott A, Bobin C. Sparse spectral unmixing for activity estimation in γ-ray spectrometry applied to environmental measurements. Applied Radiation and Isotopes 2020;156:108903.